Resonance Raman Studies of the Protocatechuate 3,4-Dioxygenase from *Brevibacterium fuscum*†

Daniel C.-T. Siu,‡ Allen M. Orville,§ John D. Lipscomb,§ Douglas H. Ohlendorf,§ and Lawrence Que, Jr.*,‡

Departments of Chemistry and Biochemistry, University of Minnesota, Minneapolis, Minnesota 55455

Received May 4, 1992; Revised Manuscript Received August 3, 1992

ABSTRACT: Resonance Raman studies of the protocatechuate 3,4-dioxygenase (PCD) from *Brevibacterium fuscum* have been carried out to take advantage of the high iron-site homogeneity of this enzyme. Native uncomplexed PCD exhibits individual resonance-enhanced ν_{CO} and δ_{CH} vibrations for the two tyrosinates coordinated to the active site iron center, which can be assigned to a particular residue by their excitation profiles. Of the two ν_{CO} features observed at 1254 and 1266 cm^{-1}, only the latter is upshifted (to 1272 cm^{-1}) when H_2O is replaced by D_2O. Similarly the 1254-cm^{-1} feature is unaffected, while the 1266-cm^{-1} feature is shifted to ~1290 cm^{-1} when inhibitors such as phenolates or terephthalate bind to the active site. These observed shifts can be rationalized by the presence of hydrogen-bonding interactions with solvent in the active site cavity, which are modulated by D_2O and eliminated upon inhibitor binding. Examination of the PCD crystal structure suggests that the axial tyrosine can be hydrogen bonded in the uncomplexed enzyme to water molecules present in the substrate binding pocket. The equatorial tyrosine may also be hydrogen bonded but to solvent molecules which are trapped in a pocket inaccessible to bulk solvent. These studies allow for the first time the association of particular Raman spectroscopic features, i.e., the ν_{CO}'s at 1254 and 1266 cm^{-1}, with the equatorial and axial tyrosine residues in the PCD active site, respectively; they lay the groundwork for further Raman studies on catalytically important species to determine the roles these tyrosine residues may play in the PCD reaction cycle.

Protocatechuate 3,4-dioxygenase (PCD) catalyzes the oxidative cleavage of protocatechuate (3,4-dihydroxybenzoate) to β-carboxy-*cis*,*cis*-muconic acid. Along with catechol 1,2-dioxygenase (CTD), PCD belongs to a class of intradiol cleaving catechol dioxygenases that have active sites consisting of a high-spin ferric ion in a non-heme ligand environment [for recent reviews, see Que (1989) and Lipscomb and Orville (1992)]. Enzymes of this type can be isolated from many widely divergent bacterial strains and are distinguished by their burgundy-red color. This characteristic color has prompted resonance Raman studies of the PCD's isolated from *Pseudomonas aeruginosa* and *Pseudomonas cepacia* and provided the first insights leading toward the proposal of endogenous tyrosyl coordination of the iron in the resting enzyme (Tatsuno et al., 1978; Felton et al., 1978, 1982; Keyes et al., 1978; Bull et al., 1979; Que & Epstein, 1981). The presence of certain resonance-enhanced Raman features is now regarded as the signature for metal–tyrosinate coordination and has engendered a subclass of metalloproteins with this structural motif (Que, 1983).

Additional spectroscopic data on PCD and CTD have led to a proposed model in which the iron is in a five-coordinate complex with two tyrosines, two histidines, and a solvent molecule (Que et al., 1976; Felton et al., 1978, 1982, 1984; Que and Epstein, 1981; Roe et al., 1984; Whittaker & Lipscomb, 1984; Pyrz et al., 1985). This proposal has recently been confirmed by the crystal structure of the PCD from *P. aeruginosa* (Ohlendorf et al., 1988), which shows the ferric active site to have the coordination environment sketched as follows:

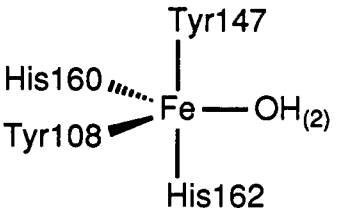

The crystallographic results show that the five iron ligands define an approximately trigonal bipyramidal geometry with the two tyrosines occupying distinct coordination sites as suggested by the Raman excitation profiles of inhibitor complexes (Que & Epstein, 1981; Pyrz et al., 1985).

The PCD from *Brevibacterium fuscum* [$(\alpha\beta Fe)_5$, 315 kDa] represents the dioxygenase with the most homogeneous iron(III) environment on the basis of the sharpness of its EPR and Mössbauer spectra (Whittaker et al., 1984). Indeed, it was the sharpness of the EPR signal that allowed the observation of ^{17}O hyperfine broadening from solvent water in the uncomplexed enzyme and provided the first evidence for solvent coordination at the iron center (Whittaker & Lipscomb, 1984). In addition, the sharp EPR spectra allowed for the observation of hyperfine broadening from ^{17}O-enriched substrate or phenolate inhibitors (Orville & Lipscomb, 1989), providing unambiguous evidence supporting the coordination of these exogenous ligands to the iron. Finally, recent EXAFS analysis of this PCD enabled us to deduce that in the resting enzyme the bound solvent is likely to be in the hydroxo form (True et al., 1990) and could thus serve as a base to deprotonate incoming substrates or inhibitors. In light of these cumulative results, the anticipated improved spectral resolution has prompted us to investigate the resonance Raman spectra of PCD isolated from *B. fuscum*. These studies, in conjunction with information from the crystal structure of *P. aeruginosa* PCD, allow us to associate Raman spectroscopic features with particular tyrosine residues in the active site and provide insight

† This work was supported by the National Institutes of Health Grants GM-33162 (L.Q.), GM-24689 (J.D.L.), and GM-46436 (D.H.O.).

‡ Department of Chemistry.

§ Department of Biochemistry.

0006-2960/92/0431-10443$03.00/0

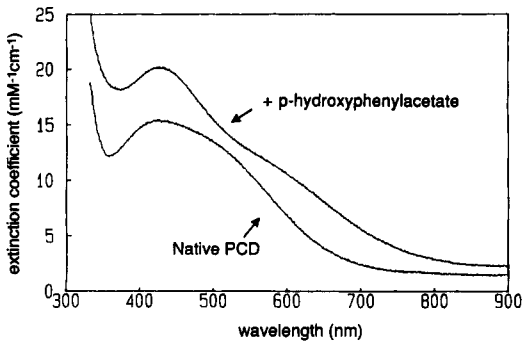

FIGURE 1: Visible spectra of *B. fuscum* PCD and its complex with *p*-hydroxyphenylacetate in 50 mM MOPS buffer, pH 7.0. Extinction coefficients are shown for the $(\alpha\beta Fe)_5$ holoprotein.

into the factors that determine the Raman properties of metal–tyrosinate proteins in general.

EXPERIMENTAL PROCEDURES

PCD was isolated from *B. fuscum* (ATCC 15993) as previously described (Whittaker et al., 1990). Samples for the resonance Raman studies were prepared in 50 mM MOPS buffer at pH 7.0 at a concentration of 0.6 mM with a consequent iron concentration of 3 mM. Enzyme–inhibitor complexes were obtained by the addition of buffered inhibitor solutions to the enzyme at 4 °C; inhibitor concentrations used were 50 mM for terephthalate, 25 mM for *p*-hydroxybenzoate, and 50 mM for *p*-hydroxyphenylacetate. D_2O samples were prepared by repeated (4×) lyophilization of the appropriate protein solution and dissolution in D_2O. D_2O (99.9% isotopic purity), $H_2{}^{18}O$ (95% isotopic purity), terephthalic acid, *p*-hydroxybenzoic acid, and *p*-hydroxyphenylacetic acid were purchased from Aldrich and used without further purification. *p*-Hydroxyphenylacetate deuteriated at the C-3′ and C-5′ positions was obtained by overnight base-catalyzed exchange at 140 °C with D_2O in a sealed NMR tube (Heistand et al., 1982).

Electronic spectra were recorded on a Cary 14 spectrophotometer. Resonance Raman spectra were obtained using a Spex Model 1403 spectrometer that was interfaced with a Spex Datamate computer for data collection and processing. Laser excitation was provided by Spectra Physics Model 171 argon ion and 375B dye (Rhodamine 6G) lasers. The Raman scattering was collected at 90° with a slit width of 4 cm^{-1}. Samples were placed in a quartz spinning cell which was cooled to ca. 5 °C by blowing cold nitrogen gas on the cell. In all samples, 0.1 M K_2SO_4 was added as an internal standard. Excitation profiles were constructed by comparing peak heights relative to the sulfate standard; no attempts were made to deconvolute overlapping features.

RESULTS AND DISCUSSION

Enzyme As Isolated. One of the more distinctive features of the intradiol cleaving catechol dioxygenases is their intense burgundy color (Fujisawa & Hayaishi, 1968), which has been attributed to the presence of tyrosinate-to-iron(III) charge transfer transitions (Tatsuno et al., 1978; Felton et al., 1978; Keyes et al., 1978; Bull et al., 1979; Que & Epstein, 1981). The visible spectrum of the PCD from *B. fuscum*, shown in Figure 1, consists of a broad absorption band with λ_{max} at 435 nm ($\epsilon \sim 3.0$ mM^{-1} cm^{-1} per Fe) and a shoulder near 525 nm. The appearance of the latter feature for the *B. fuscum* enzyme provides a clear indication that more than one visible spectral feature is present even in the uncomplexed enzyme. These

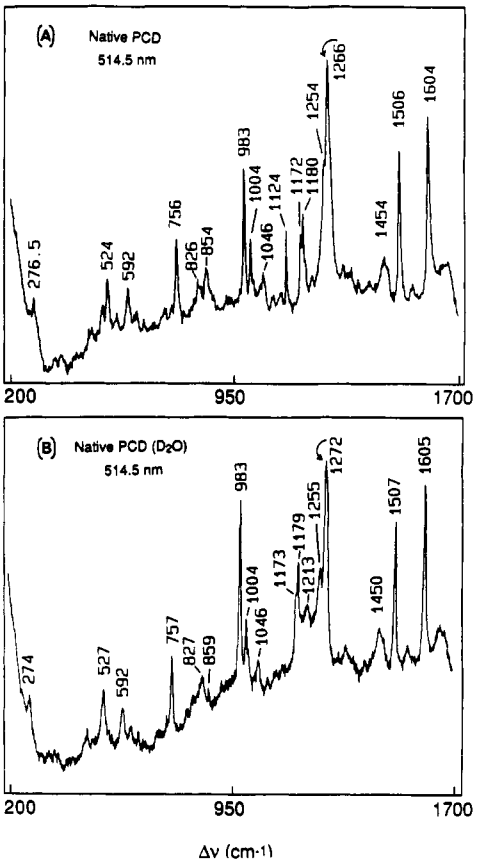

FIGURE 2: Resonance Raman spectra of *B. fuscum* PCD in (A) H_2O and (B) D_2O. Conditions: 50 mM MOPS buffer, pH 7.0; 514.5-nm laser excitation; 150 mW of power; 4-cm^{-1} slit; sum of 20 scans at 5 s/point.

features can also be discerned in the visible spectra of the PCD's from other bacteria but are not well resolved perhaps because of the greater heterogeneity of their active sites.

Ligand-to-metal charge transfer (LMCT) bands are conveniently probed by resonance Raman spectroscopy. The resonance Raman spectrum of *B. fuscum* PCD shown in Figure 2A consists of vibrational features from 200 to 1700 cm^{-1}, many of which have been previously assigned to tyrosinate deformations (Table I). Prominent in the spectrum are the signature features of tyrosinate coordination at ca. 1170, 1260, 1500, and 1600 cm^{-1}, which correspond to δ_{C-H}, ν_{CO}, and two ν_{C-C}'s, respectively (Que, 1983). Of interest is the splitting of the ν_{CO} band into two peaks at 1254 and 1266 cm^{-1} and the δ_{C-H} band into peaks at 1172 and 1180 cm^{-1}. These split features presumably arise from the two distinct tyrosinates in the active site. In studies of other PCD's (Tatsuno et al., 1978; Felton et al., 1978; Keyes et al., 1978; Bull et al., 1979; Que & Epstein, 1981), the ν_{CO} in particular has appeared asymmetric and broader than expected for a single peak, suggesting the presence of multiple components; only with the *B. fuscum* PCD have individual components become resolved. This observation supports our expectation that the *B. fuscum* PCD has the active site with least spectral heterogeneity among the catechol dioxygenases studied thus far. The Raman spectrum also includes peaks at 854 and 826 (tyrosine Fermi doublet), 756, 592 [$\nu_{Fe-O(Tyr)}$], and 524 cm^{-1}, which have been observed in earlier work and associated with other tyrosinate deformations (Tatsuno et al., 1978; Felton et al., 1978, 1982; Keyes et al., 1978; Bull et al., 1979; Que & Epstein, 1981); no splitting of these features is evident, but the lower intensities of these peaks may not allow us to discern the differences.

Table I: Resonance Raman Features (cm^{-1}) of *B. fuscum* PCD Complexes

complex	$\nu_{Fe-N(His)}$	$\nu_{Fe-O(Tyr)}$				δ_{C-H}	ν_{C-O}	ν_{C-O}	ν_{C-O}[a]	ν_{C-C}	ν_{C-C}
PCD in H_2O	276.5	524	592	756	826 854	1172 1180	1254	1266		1506	1604
PCD in D_2O	274	527	592	757	827 859	1173 1179	1255	1272		1507	1605
PCD–terephthalate		523	589	759	813 859 873	1175	1255	1290		1505	1601
PCD–*p*-hydroxybenzoate	274	526	593	756	830 856	1172	1256	1288	1278	1506	1602
PCD–PHPA		526	589	757	811 825 866	1172	1256	1288	1288	1506	1604
PCD–PHPA-d_2						1172	1256	1288	1266	1506	1604

[a] Refers to ν_{C-O} of bound phenolate inhibitor.

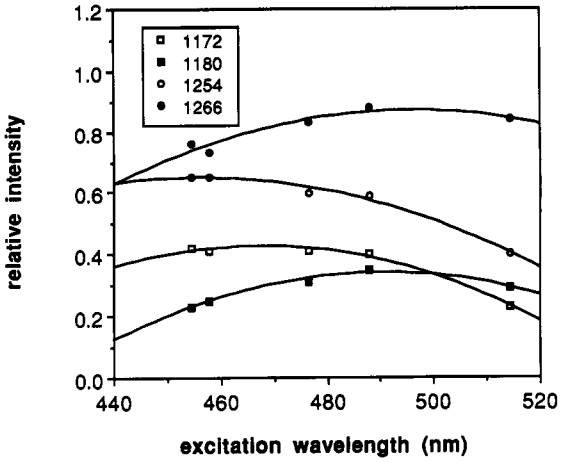

FIGURE 3: Excitation profiles for the δ_{C-H} and ν_{C-O} bands of *B. fuscum* PCD in 50 mM MOPS buffer, pH 7.0. Data points represent band peak heights relative to the 983-cm^{-1} band of SO_4^{2-}. Solid lines show second-order polynomial fits to the data.

The excitation profiles of the ν_{CO} and δ_{CH} features allow the association of individual visible absorption peaks to one of the two tyrosinates (Figure 3). The 1172- and 1254-cm^{-1} peaks exhibit maximum enhancement near 450 nm (Tyr A), while the 1180- and 1266-cm^{-1} peaks show maximum enhancement near 500 nm (Tyr B). Thus the tyrosinate with the lower energy vibrations appears to give rise to the higher energy LMCT band. The presence of two distinct tyrosine environments, each associated with a different LMCT band, is in agreement with the crystal structure of the *P. aeruginosa* PCD (Ohlendorf et al., 1988). Because equatorial ligands in a trigonal bipyramidal complex are expected to have shorter bonds than corresponding axial ligands (Kepert, 1982), the two tyrosinates in the PCD active site would be expected to give rise to tyrosinate LMCT bands of different energy.

The two tyrosines are further distinguished by their Raman behavior in D_2O buffer (Figure 2B). The 1266-cm^{-1} peak experiences a 6-cm^{-1} upshift to 1272 cm^{-1}, while the 1254-cm^{-1} ν_{CO} feature remains at essentially the same position. The tyrosinate ν_{CO} reflects the extent of double bond character associated with the phenolate C–O bond. Phenol and its conjugate base exhibit ν_{CO}'s of 1249 and 1281 cm^{-1}, respectively (Pinchas, 1972). The upshift for the 1266-cm^{-1} feature indicates that the tyrosinate associated with it is involved in hydrogen-bonding interactions and that the hydrogen-bond donor moiety is accessible to bulk solvent. The replacement of hydrogen for deuterium in the hydrogen bond would be expected to weaken the hydrogen-bonding interaction and increase the ν_{CO}. Similar upshifts have been observed for the ν_{O-O} and $\nu_{Fe-O-Fe}$ features of oxyhemerythrin in D_2O buffer and ascribed to hydrogen-bonding interactions (Shiemke et al., 1986). The low value of the 1254-cm^{-1} ν_{CO} also suggests the presence of hydrogen-bonding interactions, but its insensitivity to H_2O/D_2O exchange requires that the solvent molecules hydrogen bonded to this tyrosinate be inaccessible to bulk solvent. Alternatively, the low ν_{CO} may result from a stronger Fe–O interaction, which would mimic the effect of a proton.

There is one other feature of the spectrum of uncomplexed PCD that is affected by D_2O; the peak at 276.5 cm^{-1} downshifts to 274 cm^{-1} in D_2O. Felton et al. (1978) previously noted this peak in the spectrum of *P. aeruginosa* PCD and initially suspected it to be an Fe–S stretch; however, this possibility was eliminated by the lack of a ^{35}S effect on the spectrum (Felton et al., 1982). It was then proposed to be an Fe–N(Im) stretch; our observation of its downshift in D_2O for the *B. fuscum* enzyme supports its assignment to $\nu_{Fe-N(Im)}$. This downshift is comparable to the 2-cm^{-1} shift observed for the $\nu_{Cu-N(Im)}$ in stellacyanin (Nestor et al., 1984). It is not clear at this point whether the 276.5-cm^{-1} peak corresponds to one or both histidines in the active site. It seems likely that the axial and equatorial histidines would have different Fe–N bond strengths and thus exhibit different $\nu_{Fe-N(Im)}$ features. Unfortunately, the weak enhancement of this feature makes an excitation profile study rather difficult to carry out and prevents us from associating this feature with the tyrosinate LMCT band to which it is coupled.

We also attempted to observe Raman features that may be attributed to the coordinated solvent molecule by studying samples in $H_2{}^{18}O$ buffer. Such an isotopic substitution did not perturb the Raman spectrum of PCD, so the $Fe-OH_{(2)}$ stretching mode is apparently not coupled with the tyrosinate LMCT bands.

Effect of Inhibitors. The spectral changes elicited by the binding of inhibitors serve to corroborate and amplify the conclusions we have drawn from the study on the uncomplexed enzyme. Three inhibitor complexes were investigated: terephthalate, *p*-hydroxybenzoate, and *p*-hydroxyphenylacetate. All three inhibitors possess a carboxylate functionality analogous to that of the native substrate to enhance access to the active site. The crystal structure has suggested that Arg 133 on the α subunit serves as the locus of this carboxylate interaction (Ohlendorf et al., 1988). As was shown for the *P. aeruginosa* enzyme (Que & Epstein, 1981), terephthalate is a weak competitive inhibitor with a K_i of 6 mM and induces a red-shift in the visible spectrum affording a λ_{max} of 520 nm.

The red-shift of the λ_{max} relative to that of the uncomplexed enzyme is consistent with the replacement of the coordinated OH ligand with carboxylate. The other carboxylate presumably interacts with Arg 133. The complex exhibits a well-resolved resonance Raman spectrum with features very similar to those found in the spectrum of the uncomplexed enzyme, but the two tyrosine ν_{CO} features are now observed at 1256 and 1290 cm^{-1} (Table I). It would appear that the 1266-cm^{-1} peak has shifted to 1290 cm^{-1} in this inhibitor complex. An examination of the excitation profiles for the inhibitor complex (data not shown) reveals that the excitation maxima for the 1256- and 1290-cm^{-1} features have shifted to ~550 and >600 nm, respectively, in accordance with the red-shift of the visible spectrum relative to that of the uncomplexed enzyme. These observations agree completely with earlier data obtained on the corresponding *P. aeruginosa* PCD–terephthalate complex (Que & Epstein, 1981). With respect to the uncomplexed enzyme, bands from the two tyrosines in the terephthalate complex, although shifted, appear to retain their individual characteristics and relative energy relationships. We thus assign the 1256- and 1290-cm^{-1} features to Tyr A and B, respectively.

The phenolate inhibitors, *p*-hydroxybenzoate and *p*-hydroxyphenylacetate, competitively inhibit PCD with K_i values of 1 and 5 mM, respectively. The introduction of a CH_2 group between the carboxylate and the ring appears to lower the inhibitor affinity for the active site, perhaps as a consequence of the diminished acidity of the phenol or the longer distance between the carboxylate and phenolate oxygen resulting in a poorer overall fit in the active site. The binding of the phenolate inhibitors to the PCD iron site engenders UV–vis spectral changes due to perturbations of the tyrosinate LMCT bands and the addition of an LMCT band from the inhibitor. Indeed, the *p*-hydroxyphenylacetate complex gives rise to a more pronounced low-energy shoulder (Figure 1) than found in the uncomplexed enzyme. In contrast, the *p*-hydroxybenzoate complex shows a spectrum with only one prominent band at 432 nm (ϵ_M = 17 000 or 3.4 mM^{-1} cm^{-1} per Fe), suggesting that the lower energy tyrosinate LMCT band is blue-shifted and merged with the higher energy LMCT band.

Resonance Raman studies on these complexes show that both exogenous phenolates actually coordinate to the metal center because of the appearance of an additional ν_{CO} feature which downshifts when the corresponding ring-deuteriated derivative is used (Table I). These conclusions agree with those obtained from EPR studies of complexes with ^{17}O-labeled inhibitors (Orville & Lipscomb, 1989). In addition, the retention of the ν_{CO} features associated with the tyrosinates indicates that these endogenous ligands are not displaced when the phenolate inhibitor binds. The *p*-hydroxybenzoate complex exhibits three ν_{CO}'s at 1256, 1278, and 1288 cm^{-1}, similar to those reported for the *P. aeruginosa* enzyme inhibitor complex (Que & Epstein, 1981). The earlier study demonstrated that the 1278-cm^{-1} peak downshifted when the deuteriated inhibitor was used. The *p*-hydroxyphenylacetate complex, on the other hand, exhibits only two ν_{CO}'s at 1256 and 1288 cm^{-1}, suggesting that the ν_{CO} from PHPA overlaps with the ν_{CO} of one of the tyrosines. When the deuteriated inhibitor is used, a new feature appears at 1266 cm^{-1}, indicating that the ν_{CO} for PHPA is similar to that of Tyr B. The two inhibitors have different ν_{CO}'s because of the nature of the substituents para to the phenolate oxygen. Interestingly, as found for the terephthalate complex, only one of the two tyrosinate ν_{CO}'s is significantly shifted upon binding of either phenolate inhibitor; the ν_{CO} at 1256 cm^{-1} is essentially unaffected, while the other upshifts to 1288 cm^{-1}. These features are also unshifted when D_2O is used as solvent.

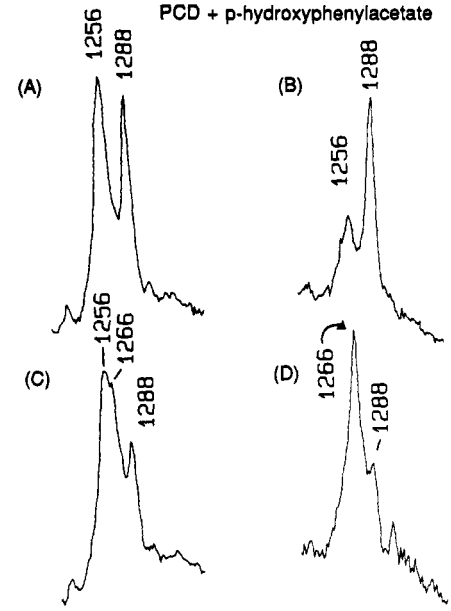

FIGURE 4: ν_{CO} region of the resonance Raman spectra of *B. fuscum* PCD complexed to *p*-hydroxyphenylacetate or its analogue deuteriated at C-3′ and C-5′ in 50 mM MOPS buffer, pH 7.0. (A) PCD–PHPA with 488-nm excitation; (B) PCD–PHPA with 578-nm excitation; (C) PCD–PHPA-d_2 with 488-nm excitation; (D) PCD–PHPA-d_2 with 593.5-nm excitation. Spectrometer conditions are as given in the legend to Figure 2.

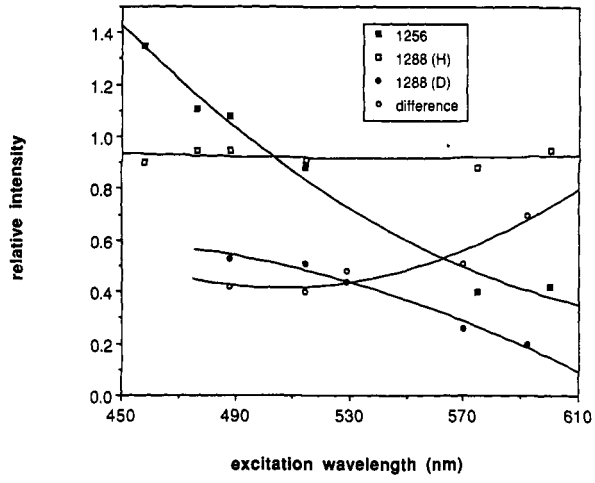

FIGURE 5: Excitation profiles for the ν_{C-O} bands of *B. fuscum* PCD complexed to *p*-hydroxyphenylacetate or its analogue deuteriated at C-3′ and C-5′ in 50 mM MOPS buffer, pH 7.0. The difference profile was obtained by subtracting the 1288-cm^{-1} profile of the deuteriated analogue from that of the protonated analogue.

The relatively well-resolved visible spectrum of the PCD–*p*-hydroxyphenylacetate complex was further probed with an excitation profile study (Figures 4 and 5) of the ν_{CO} features. For the PHPA complex, the 1256-cm^{-1} feature is maximally enhanced below 450 nm, as found for the analogous Tyr A in the uncomplexed enzyme. The 1288-cm^{-1} peak, on the other hand, has a flat profile from 450 to 600 nm, suggesting that there are two ν_{CO}'s represented by the 1288-cm^{-1} peak, each of which has a distinct excitation maximum. When the inhibitor ν_{CO} is downshifted by ring deuteriation, the ν_{CO} remaining at 1288 cm^{-1} assigned to Tyr B shows a maximum near 500 nm, a behavior similar to that of Tyr B in the uncomplexed enzyme. When the 1288-cm^{-1} profile of the PHPA-d_2 complex is mathematically subtracted from the composite 1288-cm^{-1} profile of the PHPA complex, an

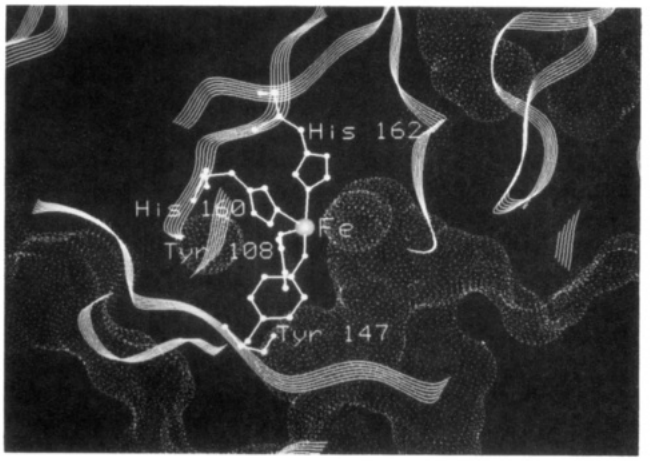

FIGURE 6: Thin slab view through the active site of PCD. The dots represent the solvent-accessible surface. The six-stranded ribbons represent the course of the polypeptide backbone of PCD. The four iron ligands are displayed as balls and sticks. Coordinates used are from the refined model of PCD from *P. aeruginosa* (D. H. Ohlendorf, manuscript in preparation).

excitation maximum is found near 600 nm (Figure 5), which we associate with the ν_{CO} of the bound PHPA. Thus the three phenolates (two tyrosines plus inhibitor) in the PHPA complex appear to give rise to LMCT bands with three different energies.

Relationship to the Active Site Structure. The resonance Raman data presented above show the presence of two distinct tyrosine residues bound to the active site iron, Tyr A associated with the smaller ν_{CO} and the higher energy LMCT band and Tyr B with the larger ν_{CO} and the lower energy LMCT band. Furthermore, the ν_{CO} of Tyr A appears insensitive to changes in the active site environment, while that of Tyr B shifts upon H_2O/D_2O exchange in the uncomplexed enzyme and upon formation of inhibitor complexes. Because of the availability of the crystal structure of PCD from *P. aeruginosa* (Ohlendorf et al., 1988), these Raman properties may afford an opportunity to associate a particular tyrosine residue in the active site with its spectroscopic features. The inherent assumption in this comparison is that the active sites of the PCD's from *P. aeruginosa* and *B. fuscum* are essentially the same; this assumption is borne out by the similarity of the spectroscopic properties of the two enzymes (Lipscomb & Orville, 1992).

Examination of the crystallographically determined active site indicates that the two coordinated tyrosines are in different environments (Figure 6). Tyrosine 108 occupies an equatorial site on the trigonal bipyramid adjacent to a solvent pocket that is isolated from bulk solvent. Tyrosine 147 occupies an axial site on the trigonal bipyramid and is in contact with bulk solvent in the active site. Solvent molecules in this region are likely to be displaced when substrates or inhibitors bind to PCD.[1] Neither tyrosine appears to be within hydrogen-bonding distance of exchangeable protons not associated with solvent. The insensitivity of Tyr A to H_2O/D_2O exchange and to inhibitor binding and the corresponding sensitivity of Tyr B to these changes compels us to assign Tyr A as the equatorial tyrosine (Tyr 108 in the *P. aeruginosa* structure) and Tyr B as the axial tyrosine (Tyr 147 in the *P. aeruginosa* structure). The Raman data clearly demonstrate that the axial tyrosine is hydrogen bonded to solvent; exchange with bulk D_2O thereby engenders the upshift observed in the spectrum of the uncomplexed enzyme. This hydrogen-bonding interaction is eliminated when inhibitors bind to the active site and displace the solvent molecules, causing the ν_{CO} of axial Tyr B to shift to $\sim$1290 cm^{-1}. On the other hand, the equatorial tyrosine with its isolated solvent pocket is insulated from changes occurring in the active site. Its low ν_{CO} value may arise from hydrogen bonding to solvent in this isolated pocket or from a stronger Fe–O bonding interaction as expected for the equatorial site of a trigonal bipyramid (Kepert, 1982).

The ν_{CO} of the bound PHPA in comparison with those of Tyr A and B in the PCD–PHPA complex provides further insight into the Raman spectra of metal–tyrosinate proteins. The inhibitor most likely binds to the equatorial coordination site occupied by the solvent in the uncomplexed enzyme (Orville & Lipscomb, 1989; Ohlendorf et al., 1988; Whittaker & Lipscomb, 1984). Tyr A, Tyr B, and PHPA are all 4-alkylphenolates and would thus be expected to have similar inherent vibrational features. Differences in phenolate vibrations observed in the resonance Raman spectrum of the PCD–PHPA complex should then result from specific interactions in the active site. Interestingly, the ν_{CO} of the equatorial PHPA is 30 cm^{-1} higher than that of equatorial Tyr A and nearly identical to that of axial Tyr B. If the strength of the Fe–O phenolate interaction were the principal factor determining the value of its ν_{CO}, then the bound PHPA and Tyr A would be expected to have similarly low ν_{CO} values, since both are coordinated in equatorial sites of a trigonal bipyramid. The observation that they are quite dissimilar suggests that some other factor principally determines the ν_{CO} value of a coordinated phenolate. The nearly identical ν_{CO}'s of Tyr B and PHPA suggest that the ν_{CO} value is determined by the extent of hydrogen bonding, the presence of which downshifts the ν_{CO} value from its phenolate maximum (ca. 1290 cm^{-1}) toward the phenol minimum (ca. 1250 cm^{-1}) (Pinchas, 1972). We suggest that the ν_{CO} of Tyr A in the PCD–PHPA complex remains at 1254 cm^{-1} because Tyr A retains its hydrogen bonding with its isolated solvent pocket, while Tyr B and the bound PHPA both exhibit ν_{CO}'s that are near the phenolate limit and insensitive to H_2O/D_2O exchange, because the binding of inhibitor has expelled potential hydrogen-bonding solvent molecules. On the basis of these observations, we suggest that the ν_{CO} value of a metal-coordinated tyrosinate provides little insight into the strength of the metal–phenolate interaction but instead may be useful for assessing the presence of hydrogen-bonding interactions to the bound tyrosinate. Raman experiments on other metal–tyrosinate proteins should be carried out to corroborate this point.

The proposed mechanism for PCD involves ligand variations and displacement during catalysis (Que, 1989; True et al., 1991; Lipscomb & Orville, 1992). Our ability to assign for the first time particular optical and Raman features to individual tyrosines in *B. fuscum* PCD by a combination of Raman observations and crystallographic arguments lays the groundwork for the further use of these spectroscopic methods to determine how the individual tyrosine residues may participate in the catalytic cycle.

[1] Analysis of electron density difference maps of monohydroxy inhibitor complexes of the PCD from *P. aeruginosa* indicate loss of crystallographically defined solvent molecules from the active site pocket. In contrast, no loss of the sequestered solvent from the vicinity of the equatorial ligands is observed in these complexes (A. M. Orville, D. H. Ohlendorf, and J. D. Lipscomb, unpublished observations).

ACKNOWLEDGMENT

We thank Dr. Bridget A. Brennan for experimental assistance.

REFERENCES

Bull, C., Ballou, D. P., & Salmeen, I. (1979) *Biochem. Biophys. Res. Commun. 87*, 836–841.

Felton, R. H., Cheung, L. D., Phillips, R. S., & May, S. W. (1978) *Biochem. Biophys. Res. Commun. 85*, 844–850.
Felton, R. H., Barrow, W. L., May, S. W., Sowell, A. L., Goel, S., Bunker, G., & Stern, E. A. (1982) *J. Am. Chem. Soc. 104*, 6132–6134.
Felton, R. H., Gordon, S. L., Sowell, A. L., & May, S. W. (1984) *Biochemistry 23*, 3955–3959.
Fujisawa, H., & Hayaishi, O. (1968) *J. Biol. Chem. 243*, 2673–2681.
Heistand, R. H., II, Lauffer, R. B., Fikrig, E., & Que, L., Jr. (1982) *J. Am. Chem. Soc. 104*, 2789–2796.
Kepert, D. L. (1982) *Inorganic Stereochemistry*, Chapters 4 and 5, Springer-Verlag, Berlin.
Keyes, W. E., Loehr, T. M., & Taylor, M. L. (1978) *Biochem. Biophys. Res. Commun. 83*, 941–945.
Lipscomb, J. D., & Orville, A. M. (1992) *Met. Ions Biol. Syst. 28*, 243–298.
Nestor, L., Larrabee, J. A., Woolery, G., Reinhammer, B., & Spiro, T. G. (1984) *Biochemistry 26*, 8059–8065.
Ohlendorf, D. H., Lipscomb, J. D., & Weber, P. C. (1988) *Nature 336*, 403–405.
Orville, A. M., & Lipscomb, J. D. (1989) *J. Biol. Chem. 264*, 8791–8801.
Pinchas, S. (1972) *Spectrochim. Acta, Part A 28*, 801.
Pyrz, J. W., Roe, A. L., Stern, L. J., & Que, L., Jr. (1985) *J. Am. Chem. Soc. 107*, 614–620.
Que, L., Jr. (1983) *Coord. Chem. Rev. 50*, 73–108.
Que, L., Jr. (1989) in *Iron Carriers and Iron Proteins* (Loehr, T. M., Ed.) pp 467–524, VCH, New York.
Que, L., Jr., & Epstein, R. M. (1981) *Biochemistry 20*, 2545–2549.
Que, L., Jr., Lipscomb, J. D., Zimmermann, R., Münck, E., Orme-Johnson, N. R., & Orme-Johnson, W. H. (1976) *Biochim. Biophys. Acta 452*, 320–334.
Roe, A. L., Schneider, D. J., Mayer, R. J., Pyrz, J. W., Widom, J., & Que, L., Jr. (1984) *J. Am. Chem. Soc. 106*, 1676–1681.
Shiemke, A. K., Sanders-Loehr, J., & Loehr, T. M. (1986) *J. Am. Chem. Soc. 108*, 2437–2443.
Tatsuno, Y., Saeki, Y., Iwaki, T., Yagi, M., Nozaki, M., Kitagawa, T., & Otsuka, S. (1978) *J. Am. Chem. Soc. 100*, 4614–4615.
True, A. E., Orville, A. M., Pearce, L. L., Lipscomb, J. D., & Que, L., Jr. (1990) *Biochemistry 29*, 10847–10854.
Whittaker, J. W., & Lipscomb, J. D. (1984) *J. Biol. Chem. 259*, 4487–4495.
Whittaker, J. W., Lipscomb, J. D., Kent, T. A., & Münck, E. (1984) *J. Biol. Chem. 259*, 4466–4475.
Whittaker, J. W., Orville, A. M., & Lipscomb, J. D. (1990) *Methods Enzymol. 188*, 82–88.